RSC Advances

PAPER

View Article Online
View Journal | View Issue

Cite this: *RSC Adv.*, 2025, **15**, 45628

Auto-luminescence study of thermal unfolding of DNA G-quadruplexes

Vladislav Yu. Kudrya, [a] Igor Ya. Dubey, [b] Valentyna V. Negrutska[b] and Antonina P. Naumenko *[a]

A new method for monitoring the unfolding of G-quadruplex DNA (G4) was proposed based on the native luminescence of the G4 system during its stepwise thermal denaturation. An antiparallel quadruplex formed by the Tel22 oligonucleotide (a fragment of human telomeric DNA) was used as a model in this study. Pre-folded G4 samples heated to various temperatures in the range of 50–90 °C were shock-frozen to trap the intermediates, and their low-temperature fluorescence and phosphorescence spectra were recorded. It was shown that effective unfolding of Tel22-G4 occurs in the region of 60–70 °C, and the process stops at temperatures above 80 °C. G4-associated fluorescence (λ = 387 nm) was found to decrease with increasing temperature, while the emission at 365 nm, corresponding to the unfolded Tel22 (and possibly to partially unfolded intermediates), increased. These spectral changes, along with the appearance of G-base emission in the Tel22 phosphorescence spectrum, are associated with the thermal denaturation of the G-quadruplex structure. A transition midpoint temperature (T_m) within 64–67 °C was obtained for Tel22-G4 from the temperature dependence of fluorescence at two wavelengths. The proposed approach allowed, for the first time, to monitor the unfolding of quadruplex DNA using its intrinsic luminescence and offered new insights into the nature of this process.

Received 8th July 2025
Accepted 5th November 2025

DOI: 10.1039/d5ra04883d

rsc.li/rsc-advances

1. Introduction

DNA G-quadruplexes (G4s) are specific four-stranded assemblies formed by the folding of some guanine-rich DNA sequences and are based on the stacks of guanine quartets (G-quartets), square planar arrangements of four guanine bases connected by non-canonical (usually Hoogsteen-type) hydrogen bonds, and stabilized by monovalent metal cations (*e.g.* Na^+ and K^+).[1–3] The structure and biological functions of DNA quadruplexes have been extensively studied over the past three decades. In particular, G4s are formed at the ends of telomeres and play a crucial biological role as elements regulating the activity of telomerase, the enzyme responsible for synthesizing telomeric DNA. Guanine-rich sequences potentially able to fold into G4 structures are found in many functionally important genome regions, particularly in gene promoters.[4,5] Stable RNA quadruplexes have also been discovered, and experimental data suggest that these structures may participate in cellular mechanisms associated with both RNA (*e.g.* mRNA processing and translation) and DNA (*e.g.* transcription and telomere elongation) processes.[6,7] Quadruplex structures are currently recognized as key regulatory elements involved in multiple biological processes, from DNA replication and gene expression to genome maintenance.[8–10]

G4 structures participate in the development of multiple pathologies, including cancer and aging. For example, telomerase, an enzyme responsible for the synthesis of telomeric DNA, is highly active in a vast majority of cancer cells, in contrast to most normal ones; thus, telomerase is a target for antitumor therapy.[11,12] G-quadruplex structures are formed in telomeric DNA by folding its terminal single-stranded region containing numerous telomeric repeats (TTAGGG in humans). Small molecules that are able to bind with and stabilize these G4 structures inhibit telomerase activity and demonstrate anticancer properties.[2,11–13] The antitumor effects of G4-DNA ligands are not only limited to telomerase inhibition but also associated with ligand-mediated DNA damage.[14,15] In general, G-quadruplex nucleic acids, both DNA and RNA, are considered promising molecular targets for anticancer therapy.[2,4,5,10,16–18]

G4 structures are characterized by broad structural diversity and include various types of parallel, antiparallel and hybrid topologies, depending on the sequence and type of stabilizing cation, the presence of ligands and other factors.[1,19,20] The folding and unfolding of G4s is a basis of their regulatory functions in the cell. Knowledge of folding/unfolding mechanisms of G-quadruplexes is essential for understanding their biological functions.

A variety of biophysical techniques have been used to investigate these processes. The π-electronic systems of G-

[a]*Faculty of Physics, Taras Shevchenko National University of Kyiv, 60, Volodymyrs'ka Str., 01033 Kyiv, Ukraine. E-mail: antonina.naumenko@knu.ua*

[b]*Institute of Molecular Biology and Genetics of the NAS of Ukraine, 150, Zabolotnogo Str., 03143 Kyiv, Ukraine*

quadruplex DNA can be studied by optical spectroscopy. For years, the main attention has been paid to optical absorption methods, such as UV-Vis and circular dichroism (CD) spectroscopy. These fast and non-destructive methods play an important role in monitoring G4 folding/unfolding and studying their kinetics and thermodynamics. UV spectroscopy is the most common approach for studying nucleic acids, including G-quadruplexes. G4 unfolding can be easily monitored by the thermal denaturation ("UV melting") method.[21–29] In addition, thermal difference absorption spectra allow discriminating between various quadruplex topologies.[30,31] Circular dichroism spectroscopy is another common biophysical method for the study of G4 topology, folding and ligand binding. CD is sensitive to biomolecule conformation, and G4s with different topologies exhibit distinct spectroscopic signatures.[23,26–28,32–36]

Fluorescence-based methods are based on the introduction of fluorophores into the structure of G-forming sequences. Thermal denaturation profiles of model quadruplexes have been studied by substituting adenine residues with the fluorescent analogue 2-aminopurine.[26,35] Besides the intrinsic fluorescence of 2-aminopurine, the emission of covalently attached fluorescent dyes can be used to follow structural changes associated with folding/unfolding. Covalent labeling of the 3′- and 5′-ends of oligonucleotide with a suitable pair of donor and acceptor fluorophores, *e.g.* 6-carboxyfluorescein (FAM) and (tetramethylrhodamine (TAMRA)), allows to investigate the unfolding pathways through FRET (Fluorescence Resonance Energy Transfer) melting experiments. Structural changes and the formation of folding intermediates manifest themselves as a change in the distance and orientation between the dyes that influence FRET efficiency.[26,35] A quencher-free, FRET-like assay has recently been proposed to investigate the process of G4 folding.[37]

In recent years, single-molecule techniques have been employed to study the kinetics and thermodynamics of quadruplex folding/unfolding.[38] In particular, single-molecule FRET (smFRET) microscopy has been used to obtain a direct view of the folding and underlying conformational dynamics of fluorescently labeled G4s formed by the human telomeric sequence.[39–41]

Mechanical unfolding of G4 by magnetic tweezers (single-molecule force spectroscopy) allows direct observation of sequential folding pathways and transitions between intermediates. In this approach, the immobilized quadruplex-forming oligonucleotide is terminally attached to a magnetic bead, and G4 unfolding is forced by a magnetic field.[42–46]

Magnetic tweezers have also been successfully integrated with fluorescence spectroscopy to study folding/unfolding equilibria. In this approach based on FRET effect, a quadruplex-forming sequence is labeled with a pair of donor and acceptor fluorescent dyes (such as Cy3 and Cy5 cyanines) and used with a magnetic tweezer. In this case, the dependence of FRET on the applied mechanical unfolding force is monitored.[47–50]

The native low-intensity fluorescence of DNA at ambient temperature can also be detected by sensitive spectrofluorimeters.[51,52] In particular, intrinsic fluorescence in combination with NMR has been used to study G-quadruplex formation.[51]

Thermal denaturation of G4s has also been studied by calorimetry techniques,[23,53–55] mass spectrometry,[56] and, recently, time-resolved small-angle X-ray scattering.[57]

Computational approaches are currently widely used to model the processes of quadruplex folding and unfolding. Modeling is mainly based on molecular dynamics simulations.[58–62] These studies have proposed numerous folding/unfolding pathways, possible mechanisms of interconversion between various topological forms of G-quadruplexes and the structures of transition intermediates.

Environment-sensitive fluorescence methods are the methods of choice to study structural changes in biomolecules, including their folding and unfolding processes. However, common approaches that are based on the introduction of fluorophores, either fluorescent dyes or fluorescent nucleoside analogs, are somewhat "artificial", as the introduced molecular moieties can affect the structure and biophysical properties of G-quadruplexes. Therefore, it is of great interest to study the intrinsic luminescence of native G4s. There is a gap in the knowledge of the auto-luminescence (both fluorescence and phosphorescence) properties of G4 structures that can be observed at low temperatures, and their temperature dependence associated with folding/unfolding of G4 assemblies.

We have previously shown that the specific optical properties of quadruplex DNA and their environment-dependent changes allow its sensing based on auto-luminescence.[63–65] This approach does not require the presence of additional fluorophores and uses the native fluorescence/phosphorescence of DNA. Here, we studied the spectral properties (optical absorption, auto-fluorescence, and auto-phosphorescence) of the Tel22 oligonucleotide capable of forming a G-quadruplex structure. The effects observed in our label-free fluorescence and phosphorescence experiments are associated with the thermal unfolding of G4.

2. Experimental methods

2.1 Materials

HPLC-purified deoxyoligonucleotides d[AGGG(TTAGGG)$_3$] (Tel22), the model sequence d[CCCGGGTTTAAA] previously designed to study singlet and triplet excitation in DNA,[63,64,66] and pentadecathymidylate (dT)$_{15}$ were obtained from Eurogentec (Belgium). Salmon sperm DNA was purchased from Roth (Germany), and 2′-deoxyguanosine 5′-monophosphate (dGMP) was obtained from Sigma (USA).

Oligonucleotide concentrations were determined spectrophotometrically in aqueous solution using the following calculated extinction coefficients ε_{260}: 2.28×10^5 M^{-1} cm^{-1} for Tel22, 1.22×10^5 M^{-1} cm^{-1} for (dT)$_{15}$, 1.16×10^5 M^{-1} cm^{-1} for d d[CCCGGGTTTAAA]. The concentration of dGMP in water was 1.5×10^{-4} M.

A 100 μM solution of Tel22 was prepared in 10 mM sodium cacodylate buffer (pH 7.3) containing 100 mM NaCl. This solution was used for oligonucleotide folding and all

fluorescence and phosphorescence measurements. UV absorption spectra were recorded using 5 μM oligonucleotide samples in the same buffer.

2.2. Quadruplex preparation and thermal unfolding

The antiparallel Tel22 quadruplex (Tel22-G4) was prepared as described in ref. 67. Briefly, a 100 μM oligonucleotide solution in the above-mentioned cacodylate buffer was heated at 95 °C for 5 min and then slowly cooled to room temperature over 10 h to form the required G-quadruplex structure and left at 4 °C overnight for equilibration. The obtained solution of Tel22-G4 was stored at this temperature.

For the G4 unfolding dynamics studies, two types of Tel22 samples were investigated: (1) G4-folded Tel22 (Tel22-G4) samples that were frozen to $T = 77$ K immediately before measurement; (2) Tel22-G4 samples heated to various temperatures (in the range of 50–90 °C, in 10 °C increments) for 3 min and subsequently shock-frozen to $T = 77$ K by immersing in liquid nitrogen immediately before measurement.

2.3. Spectral measurements

Optical absorption spectra were recorded at room temperature using a Cary 60 UV-Vis spectrophotometer (Agilent, USA). Fluorescence and phosphorescence (excitation and emission) spectra were recorded on a Cary Eclipse fluorescence spectrophotometer (Varian, Australia). Fluorescence spectra were obtained at room temperature and at $T = 77$ K, while phosphorescence spectra were measured only at $T = 77$ K. Excitation was provided by a xenon lamp. The spectral slit widths for excitation and emission were set to 5 nm for fluorescence and 10 nm for phosphorescence. Optical spectroscopy experiments were performed as described in ref. 63–66. Measurements at room temperature were carried out in a standard quartz cuvette with a 10 mm pathlength, whereas those at $T = 77$ K were carried out in a round aluminum cuvette (which exhibited no optical response upon excitation in the wavelength range of $\lambda = 250$–350 nm). The cuvette with a sample was shock-frozen in liquid nitrogen for 1 min and placed inside an Optistat DN cryostat (Oxford Instruments, UK) filled with liquid nitrogen. The temperature (77 K) was maintained using an Intelligent Temperature Controller ITC503S (Oxford Instruments).

Fluorescence and phosphorescence spectra were corrected for the wavelength response of the system. Excitation wavelengths were chosen using the maxima observed in the optical absorption spectra. The measurement errors for optical density, fluorescence/phosphorescence intensity and wavelength were within the standard limits of the respective equipment. The accuracy parameters for the Cary 60 UV-Vis spectrophotometer were as follows: spectral bandwidth, 1.5 nm; wavelength accuracy, ±0.5 nm. The same parameters for the Cary Eclipse fluorescence spectrophotometer were as follows: spectral bandwidth, 5 nm (fluorescence) and 10 nm (phosphorescence); wavelength accuracy, ±1.5 nm. The reproducibility of optical density (Cary 60) and fluorescence/phosphorescence intensity (Cary Eclipse) magnitudes was within 3%.

3. Results and discussion

DNA oligonucleotides containing guanine repeat sequences can fold into more compact G-quadruplex structures in the presence of some metal ions (*e.g.* Na^+ and K^+). It should be noted that four-stranded G4 structures are formed by the reversible folding of single-stranded sequences, and interconversion between various topologies is possible, which proceeds *via* various intermediate states. Both G4 folding and unfolding are complicated processes of deep structural changes that proceed *via* multiple transition states and involve the formation of a broad range of molecule conformations, partially folded regions and various arrangements of nucleotide bases.[40–42,57–62] In particular, G-triplex and G-hairpin intermediates are supposed to be involved in the multi-pathway folding of human telomeric G-quadruplex.[40] In this research, we studied the unfolding of G-quadruplex using low-temperature DNA autoluminescence.

3.1. G-quadruplex formation and thermal unfolding

The Tel22 oligonucleotide d[AGGG(TTAGGG)$_3$], a 22-mer fragment of human telomeric DNA containing three telomeric repeats (TTAGGG), was used as a model. We investigated the intrinsic fluorescence and phosphorescence (at 77 K) of Tel22 samples folded into the G4 structure and then thermally unfolded by heating to various temperatures (323–363 K), followed by shock-freezing in liquid nitrogen to trap the intermediates.

G4 was formed by folding the single-stranded Tel22 in 10 mM sodium cacodylate buffer containing 100 mM NaCl (pH 7.3). It is well established that, in the presence of Na^+ cations, Tel22 forms an intramolecular G-quadruplex with an antiparallel (basket-type) topology (Protein Data Bank code 143D).[1,68] The formation of the G4 structure is associated with the appearance of significant optical absorption at 295–300 nm corresponding to structures containing stacked G-quartets, in contrast to single- or double-stranded DNA. Thus, UV spectroscopy allows the discrimination of the G4 structure from unfolded (linear) forms and provides information on quadruplex stability. G4 folding/unfolding can be monitored by recording absorbance at 295 nm.[21,23,69]

A significant absorption at 295 nm associated with G4 was observed in the UV absorption spectra of all Tel22-G4 samples, in contrast to the (dT)$_{15}$ oligomer, which cannot form quadruplex structures (Fig. 1). Upon thermal denaturation of G4, the hyperchromism of the 260 nm band was observed; this effect is common for double-stranded nucleic acids and results from duplex unwinding and strand separation, *i.e.* the disruption of π–π-stacked, H-bonded base pairs. At the same time, the G4-specific absorption at 295 nm decreased with increasing temperature due to the gradual disappearance of the quadruplex structure (data not shown). These effects are in full agreement with the literature.[21,23,25]

Pre-folded Tel22-G4 samples were heated to various temperatures (from 50 to 90 °C, in 10 °C increments). Equilibrium sets of various unfolding intermediates are formed,

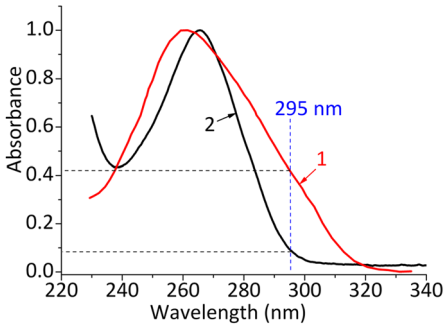

Fig. 1 Normalized absorption spectra of Tel22-G4 (1) and $(dT)_{15}$ (2). Oligonucleotide concentration: 5×10^{-6} M in 10 mM sodium cacodylate buffer containing 100 mM NaCl (pH 7.3).

depending on the temperature. After heating, the samples were shock-frozen in liquid nitrogen, which allowed trapping the transition products and intermediates to obtain their luminescence spectra. In such a way, the process of sequential G4 unfolding can be directly examined.

3.2. Fluorescence spectra

The main data on the thermal unfolding of Tel22-G4 were obtained using luminescence excitation at $\lambda = 310$ nm, where individual nucleotides do not absorb, and, as shown in our previous work,[63] only G4 structures absorb. The results of the fluorescence experiments with various molecular systems (oligonucleotides, nucleotides and DNA) are shown in Fig. 2.

Fluorescence spectra of the starting G4-folded Tel22 sample, as well as those of Tel22-G4 samples heated to 50 °C and 60 °C, coincide within experimental error. Thus, no structural changes occurred in the G-quadruplex at temperatures below 60 °C. On the other hand, fluorescence spectra of Tel22-G4 samples heated to 70 °C, 80 °C and 90 °C coincide with each other, but both positions and shapes of the bands differ from those observed at temperatures below 60 °C. Only the band associated with G4 emission ($\lambda = 387$ nm)[63] was observed in the fluorescence spectra of the starting Tel22-G4 and the samples heated to 50 °C and 60 °C. However, a new structured band ($\lambda = 365$ nm) related to the unfolded Tel22 (with a possible contribution of the emission of some amount of partially unfolded G-intermediates, such as G-triplexes or G-hairpins) was observed in the fluorescence spectra of samples heated to 70 °C, 80 °C and 90 °C. These bands were not observed in the fluorescence spectra of deoxyguanosine nucleotide, salmon sperm DNA and the model non-G4-forming oligonucleotide d[CCCGGGTTTAAA] (Fig. 2A). For comparison, the sum (superposition) of the spectra of individual nucleotides dTMP, dAMP and dGMP taken in a molar ratio of 2 : 1 : 3 corresponding to the telomeric repeat sequence d[TTAGGG] is also presented (Fig. 2B, curve 8); this ratio is close to the nucleotide ratio in the Tel22 oligonucleotide. Spectra (7) and (8) in Fig. 2B illustrate that the separate G, T and A nucleotides are not the main singlet exciton traps in the Tel22-G4 system.

Spectral data (the maxima of fluorescence bands) for the studied systems are presented in Table 1.

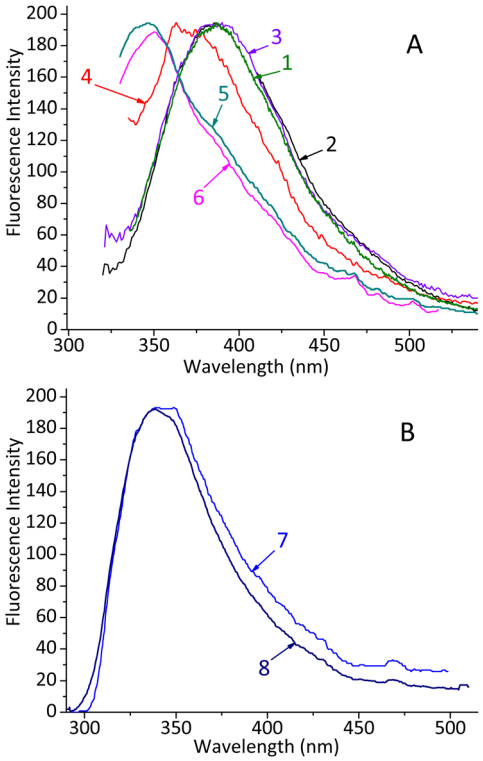

Fig. 2 Normalized fluorescence spectra of (A) Tel22-G4 (folded, non-heated) (1); Tel22 samples heated to 50 °C (2), 60 °C (3), 70 °C and above (4); control oligonucleotide d[CCCGGGTTTAAA] (5); and salmon sperm DNA (6) ($\lambda_{ex} = 310$ nm) and (B) dGMP (7) and sum of the spectra of nucleotides in a molar ratio corresponding to the sequence d[TTAGGG] (8) ($\lambda_{ex} = 260$ nm). Measurements were performed at $T = 77$ K. Spectra in panels A and B were normalized against the fluorescence of Tel22-G4 at 387 nm and 50 °C.

The intensity of the G4-associated fluorescence band at 387 nm decreased with increasing temperature, whereas the intensity of the band at 365 nm, which corresponds to the unfolded oligonucleotide, increased. Sharp changes in Tel22-G4 fluorescence occurred primarily between 60 and 70 °C. The temperature dependence of the fluorescence intensities of these two bands demonstrates that in the range 60–65 °C, the effective thermal unfolding of the G4 structure starts at temperatures above *ca.* 80 °C, and the unfolding process is practically over. Fig. 3 shows the effect of temperature on the intensities of these fluorescence bands. The curves demonstrate the gradual disappearance of the G4 system upon heating, with an increase in the content of the unfolded product (which obviously occurs *via* the formation of some unfolding intermediates).

From both thermal denaturation curves, the melting point of Tel22-G4, *i.e.* the transition midpoint temperature (T_m) for the transformation of the G-quadruplex into the single-stranded oligonucleotide, was found to be in the range of 64–67 °C. The observed temperature dependence of the fluorescence intensities at 365 and 387 nm (Fig. 3) is in a good agreement with optical absorption data ("UV melting") at $\lambda = 295$ nm and $\lambda = 260$ nm previously obtained for this quadruplex,[21,25,26,69] as well as with data obtained from G4 unfolding monitored by CD

Table 1 Fluorescence band maxima of the investigated molecular systems[a]

System (Fig. 2)	1	2	3	4	5	6	7	8
λ_{fl}, nm	387	387	387	365	338, 345	338, 350	338, 345	338, 345

[a] Spectra were recorded at 77 K with λ_{ex} = 310 nm (1–6) or 260 nm (7 and 8).

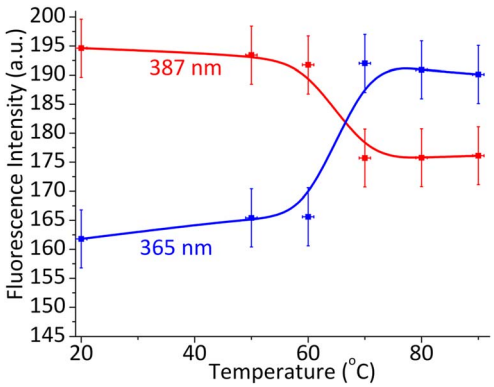

Fig. 3 Temperature dependence of the intensities of Tel22-G4 fluorescence bands with maxima at 365 and 387 nm (curve fitting was performed using the standard spline method).

spectroscopy.[23,26,28,35] In general, previous studies using well-established biophysical techniques have also demonstrated that Tel22-G4, upon heating in the same solution (100 mM Na^+), starts to quickly unfold in the region of ~55–60 °C, and at temperatures above ~70 °C, the melting curves reach a plateau, indicating the formation of the unfolded structure.

An advantage of low-temperature fluorescence is that the spectral profiles of the G4 and unfolded structure are well separated ($\Delta\lambda_{fl}$ = 22 nm). In contrast, at room temperature, the intrinsic fluorescence of G4s (in a K^+ buffer, excitation at 265 nm) decreases upon heating due to unfolding, but the emission maximum (330 nm) does not shift over the range of 20–90 °C.[51]

3.3. Phosphorescence spectra

The phosphorescence spectra of the studied systems obtained at T = 77 K are shown in Fig. 4 and 5. The phosphorescence of all the samples of Tel22, as well as the control oligonucleotide d[CCCGGGTTTAAA] and DNA macromolecule, when excited in the wavelength range of λ = 260–290 nm (Fig. 4), consisted of one wide, unstructured band (with a maximum at λ = 450 nm). This emission originates from exciplexes formed by A and T bases, as previously established for Tel22 and a number of model oligonucleotides.[63,64,66]

The phosphorescence spectra of the initial Tel22-G4 quadruplex and Tel22-G4 samples heated to 50 °C, 60 °C, 70 °C and above and excited at 260–290 nm, practically coincided within the experimental error; this phosphorescence was the result of the emission of AT-complexes only.

At the same time, the phosphorescence bands of Tel22-G4 samples heated to 70 °C, 80 °C and 90 °C, but excited at λ_{ex} = 310 nm (Fig. 5, spectrum 1), exhibit a shoulder at 390–450 nm, which presumably corresponds to unbound guanine bases (see the dGMP spectrum for comparison, with the first two maxima at λ = 398 nm and λ = 422 nm). The appearance of G-bases shoulder in the spectrum indicates that some guanine residues are excluded from G-quartets as the temperature increases. Thus, the phosphorescence in this case is a combination of emissions from AT-complexes and G-bases separated from the quadruplex structure due to the unfolding process. In contrast, the phosphorescence of Tel22-G4 samples heated to 50 and 60 °C (or unheated) and excited at λ = 310 nm corresponds solely to the emission of AT-complexes, *i.e.* only the folded G4 structure is present (Fig. 5, spectrum 2).

Thus, low-temperature phosphorescence, just as fluorescence, can be used to monitor the unfolding process of G-quadruplex DNA. In addition, the phosphorescence spectra evidence that G-intermediates, such as G-triplex and/or G-duplex (G-hairpin) structures, can be additional triplet exciton traps during G4 unfolding.

A scheme of Tel22-formed G-quadruplex unfolding with increasing temperature is shown in Fig. 6.

The main photophysical processes that take place in Tel22 oligonucleotide samples (folded Tel22-G4 and unfolded Tel22) are shown in Fig. 7. The positions of the first excited singlet (S_1) and triplet (T_1) energy levels (0–0 transition) were estimated by a well-known method:[70] the S_1 level is located at the intersection of the curves of optical absorption spectrum and fluorescence spectrum, while the T_1 level is located at the short-wavelength edge of the phosphorescence spectrum. In folded Tel22-G4, under the excitation of G4 (λ_{ex} = 310 nm; individual nucleotides do not absorb at this wavelength), singlet excitons are trapped and deactivated by fluorescence emission with λ_{max} =

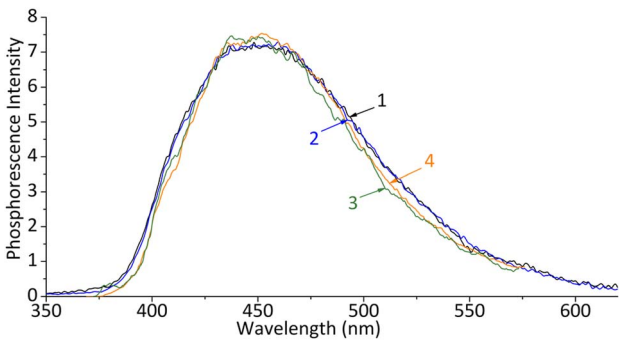

Fig. 4 Normalized phosphorescence spectra of Tel22 samples (coinciding for non-heated Tel22-G4 and Tel22-G4 samples heated to 50 °C, 60 °C, 70 °C and above) excited at λ_{ex} = 260 nm (1) and λ_{ex} = 290 nm (2); control oligonucleotide d[CCCGGGTTTAAA] (λ_{ex} = 260 nm) (3); DNA (λ_{ex} = 260 nm) (4). T = 77 K.

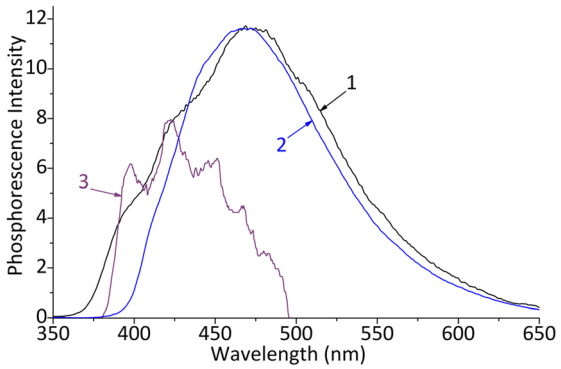

Fig. 5 Phosphorescence spectra of Tel22-G4 samples heated to 70 °C and above (1); Tel22-G4 samples heated to 50 and 60 °C or unheated (2) (λ_{ex} = 310 nm); and dGMP (3) (λ_{ex} = 260 nm). T = 77 K.

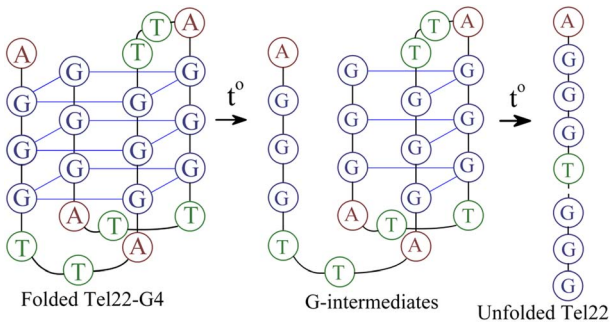

Fig. 6 Schematic of the thermal unfolding of the antiparallel G-quadruplex formed by the Tel22 oligonucleotide. Only one intermediate structure from a diverse set of possible transition intermediates is shown.

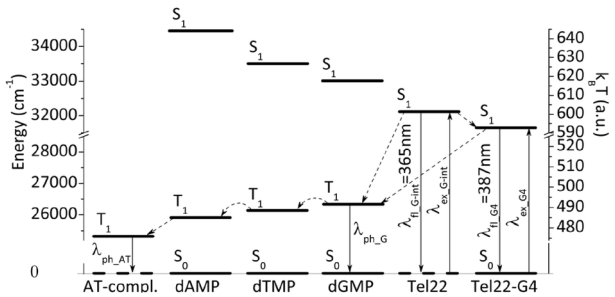

Fig. 7 General scheme of the photophysical processes in the Tel22 oligonucleotide.

387 nm. In the unfolded Tel22 oligonucleotide, under the excitation of the G-intermediates (mentioned above), singlet excitons are trapped and deactivated by fluorescence emission with λ_{max} = 365 nm. Triplet excitons (generated *via* intercombination conversion) are trapped by AT-complexes (in Tel22-G4) or both AT-complexes and G-bases (in unfolded Tel22) and deactivated by phosphorescence emission with λ_{max} = 450 nm for AT-complexes and λ_{max} = 425 nm for G-bases.

4. Conclusions

The effects observed in both the fluorescence and phosphorescence spectra (the sharp changes of fluorescence intensities in the temperature range of 60–70 °C, the appearance of a new fluorescence band at 365 nm and the G-base emission band in Tel22-G4 phosphorescence) are associated with the thermal unfolding of the G-quadruplex structure. The results were obtained using a novel experimental approach based on the study of singlet and triplet exciton traps. These results are in good agreement with data on G4 folding/unfolding obtained by other experimental techniques and computational methods and correspond to previously proposed unfolding models that involve the formation of G-triplex and G-hairpin intermediates.[40–42,60–62,71–73] At the same time, the developed approach based on a stepwise G4 unfolding and trapping of its intermediates is a direct, label-free (auto-luminescent) method that can provide information often unavailable by common biophysical methods.

The proposed approach can also be useful for studying quadruplex DNA interactions with ligands, including non-fluorescent and non-UV-absorbing compounds, whose complexes with biomolecules are rather challenging objects for spectral studies. The products and intermediates of various temperature- and time-dependent dynamic processes in other nucleic acids (single- and double-stranded DNA and RNA) can be captured as well by the reported shock-freezing technique. For example, folding/unfolding, oligonucleotide hybridization, complex formation, thermal denaturation, and unwinding can potentially be investigated by this approach.

Author contributions

Vladislav Yu. Kudrya: methodology, investigation and writing – original draft; Igor Ya. Dubey: writing – review & editing, methodology, data analysis; Valentyna V. Negrutska: methodology, investigation; Antonina P. Naumenko: investigation, data curation, data analysis and writing – review & editing.

Conflicts of interest

The authors declare that they have no competing financial or personal interests.

Data availability

All data associated with this manuscript will be available from the corresponding author upon reasonable request.

References

1 S. Burge, G. N. Parkinson, P. Hazel, A. K. Todd and S. Neidle, *Nucleic Acids Res.*, 2006, **34**, 5402–5415.
2 S. Neidle, *J. Med. Chem.*, 2016, **59**, 5987–6011.
3 K. Sato and P. Knipscheer, *DNA Repair*, 2023, **130**, 103552.
4 R. Hänsel-Hertsch, M. Di Antonio and S. Balasubramanian, *Nat. Rev. Mol. Cell Biol.*, 2017, **18**, 279–284.

5 R. Rigo, M. Palumbo and C. Sissi, *Biochim. Biophys. Acta Gen. Subj.*, 2017, **1861**, 1399–1413.
6 A. Cammas and S. Millevoi, *Nucleic Acids Res.*, 2017, **45**, 1584–1595.
7 W. Kotkowiak, C. Roxo and A. Pasternak, *ACS Med. Chem. Lett.*, 2023, **14**, 35–40.
8 D. Rhodes and H. J. Lipps, *Nucleic Acids Res.*, 2015, **43**, 8627–8637.
9 J. Spiegel, S. Adhikari and S. Balasubramanian, *Trends Chem.*, 2020, **2**, 123–136.
10 M. C. Dell'Oca, R. Quadri, G. M. Bernini, L. Menin, L. Grasso, D. Rondelli, O. Yazici, S. Sertic, F. Marini, A. Pellicioli, M. Muzi-Falconi and F. Lazzaro, *Int. J. Mol. Sci.*, 2024, **25**, 3162.
11 A. N. Guterres and J. Villanueva, *Oncogene*, 2020, **39**, 5811–5824.
12 J. Gao and H. A. Pickett, *Nat. Rev. Cancer*, 2022, **22**, 515–532.
13 L. Chen, J. Dickerhoff, S. Sakai and D. Yang, *Acc. Chem. Res.*, 2022, **55**, 2628–2646.
14 D. Hasegawa, S. Okabe, K. Okamoto, I. Nakano, K. Shin-ya and H. Seimiya, *Biochem. Biophys. Res. Commun.*, 2016, **471**, 75–81.
15 J. F. Moruno-Manchon, E. C. Koellhoffer, J. Gopakumar, S. Hambarde, N. Kim, L. D. McCullough and A. S. Tsvetkov, *Aging*, 2017, **9**, 1957–1970.
16 Quadruplex Nucleic Acids as Targets for Medicinal Chemistry, *Annu. Rep. Med. Chem.*, ed. S. Neidle, 2020, vol. 54, p. 564, ISBN: 9780128210178.
17 D. Sumanta and A. C. Pratap, *Curr. Drug Discov. Technol.*, 2022, **19**, e140222201110.
18 E. Mendes, I. M. Aljnadi, B. Bahls, B. L. Victor and A. Paulo, *Pharmaceuticals*, 2022, **15**, 300.
19 M. Kaushik, S. Kaushik, A. Bansal, S. Saxena and S. Kukreti, *Curr. Mol. Med.*, 2011, **11**, 744–769.
20 M. Farag and L. Mouawad, *Nucleic Acids Res.*, 2024, **52**, 3522–3546.
21 J.-L. Mergny, A. T. Phan and L. Lacroix, *FEBS Lett.*, 1998, **435**, 74–78.
22 A. T. Phan and J.-L. Mergny, *Nucleic Acids Res.*, 2002, **30**, 4618–4625.
23 C. M. Olsen and L. A. Marky, *Methods Mol. Biol.*, 2010, **608**, 147–158.
24 P. Changenet-Barret, Y. Hua and D. Markovitsi, *Top. Curr. Chem.*, 2015, **356**, 183–201.
25 Y. Zhang, J. Chen, H. Ju and J. Zhou, *Biochimie*, 2019, **157**, 22–25.
26 R. D. Gray, R. Buscaglia and J. B. Chaires, *J. Am. Chem. Soc.*, 2012, **134**, 16834–16844.
27 L. Ying, J. J. Green, H. Li, D. Klenerman and S. Balasubramanian, *Proc. Natl. Acad. Sci. U. S. A.*, 2003, **100**, 14629–14634.
28 Md. M. Islam, S. Fujii, S. Sato, T. Okauchi and S. Takenaka, *Molecules*, 2015, **20**, 10963–10979.
29 S. Carrino, C. D. Hennecker, A. C. Murrieta and A. Mittermaier, *Nucleic Acids Res.*, 2021, **49**, 3063–3076.
30 J.-L. Mergny, L. Lacroix, S. Amrane and J. B. Chaires, *Nucleic Acids Res.*, 2005, **33**, e138.
31 A. I. Karsisiotis, N. M. Hessari, E. Novellino, G. P. Spada, A. Randazzo and M. Webba da Silva, *Angew Chem. Int. Ed. Engl.*, 2011, **50**, 10645–10648.
32 S. Paramasivan, I. Rujan and P. H. Bolton, *Methods*, 2007, **43**, 324–331.
33 M. Vorlíčková, I. Kejnovská, J. Sagi, D. Renčiuk, K. Bednářová, J. Motlová and J. Kypr, *Methods*, 2012, **57**, 64–75.
34 A. Marchand and V. Gabelica, *Nucleic Acids Res.*, 2016, **44**, 10999–11012.
35 R. D. Gray, J. O. Trent and J. B. Chaires, *J. Mol. Biol.*, 2014, **426**, 1629–1650.
36 M. Moriya, T. Oyama, M. Goto, K. Ikebukuro and W. Yoshida, *STAR Protoc.*, 2025, **6**, 103646.
37 Z. Parada, T. G. Hoog, K. P. Adamala and A. E. Engelhart, *ACS Omega*, 2025, **10**, 3176–3181.
38 M. Lamperti, R. Rigo, C. Sissi and L. Nardo, *Photonics*, 2024, **11**, 1061.
39 M. Aznauryan, S. Søndergaard, S. L. Noer, B. Schiøtt and V. Birkedal, *Nucleic Acids Res.*, 2016, **44**, 11024–11032.
40 X.-M. Hou, Y.-B. Fu, W.-Q. Wu, L. Wang, F.-Y. Teng, P. Xie, P.-Y. Wang and X.-G. Xi, *Nucleic Acids Res.*, 2017, **45**, 11401–11412.
41 M. Basu, A. Mainan, S. Roy and P. P. Mishra, *Phys. Chem. Chem. Phys.*, 2025, **27**, 7104–7119.
42 W. Li, X.-M. Hou, P.-Y. Wang, X.-G. Xi and M. Li, *J. Am. Chem. Soc.*, 2013, **135**, 6423–6426.
43 H.-P. Ju, Y.-Z. Wang, J. You, X.-M. Hou, X.-G. Xi, S.-X. Dou, W. Li and P.-Y. Wang, *ACS Omega*, 2016, **1**, 244–250.
44 N. Li, J. Wang, K. Ma, L. Liang, L. Mi, W. Huang, X. Ma, Z. Wang, W. Zheng, L. Xu, J.-H. Chen and Z. Yu, *Nucleic Acids Res.*, 2019, **47**, e86.
45 Y. Zhang, Y. Cheng, J. Chen, K. Zheng and H. You, *Nucleic Acids Res.*, 2021, **49**, 7179–7188.
46 Y. Cheng, Y. Zhang and H. You, *Biomolecules*, 2021, **11**, 1579.
47 X. Long, J. W. Parks, C. R. Bagshaw and M. D. Stone, *Nucleic Acids Res.*, 2013, **41**, 2746–2755.
48 J. Mitra, M. A. Makurath, T. T. M. Ngo, A. Troitskaia, Y. R. Chemla and T. Ha, *Proc. Natl. Acad. Sci. USA*, 2019, **116**, 8350–8359.
49 D. A. Nicholson and D. J. Nesbitt, *J. Phys. Chem. B*, 2023, **127**, 6842–6855.
50 H. Peng, Y. Zhang, Q. Luo, X. Wang and H. You, *Biophys. Rep.*, 2024, **10**, 180–189.
51 N. T. Dao, R. Haselsberger, M.-E. Michel-Beyerle and A. T. Phan, *FEBS Lett.*, 2011, **585**, 3969–3977.
52 A. Bednarz, R. T. Rosendal, L. M. Lund and V. Birkedal, *Biochimie*, 2024, **227**, 61–67.
53 C. M. Olsen, W. H. Gmeiner and L. A. Marky, *J. Phys. Chem. B*, 2006, **110**, 6962–6969.
54 B. Pagano, A. Randazzo, I. Fotticchia, E. Novellino, L. Petraccone and C. Giancola, *Methods*, 2013, **64**, 43–51.
55 A. Garabet, L. Liu and T. V. Chalikian, *J. Chem. Phys.*, 2023, **159**, 055101.
56 A. Marchand, F. Rosu, R. Zenobi and V. Gabelica, *J. Am. Chem. Soc.*, 2018, **140**, 12553–12565.

57 R. C. Monsen, T. M. Sabo, R. Gray, J. B. Hopkins and J. B. Chaires, *Nucleic Acids Res.*, 2025, **53**, gkaf043.
58 D. Luo and Y. Mu, *J. Phys. Chem. B*, 2016, **120**, 4912–4926.
59 T. Panczyk, P. Wojton and P. Wolski, *Biophys. Chem.*, 2019, **250**, 106173.
60 P. Stadlbauer, V. Mlýnský, M. Krepl and J. Šponer, *J. Chem. Inf. Model.*, 2023, **63**, 4716–4731.
61 Z. Zhang, V. Mlýnský, M. Krepl, J. Šponer and P. Stadlbauer, *J. Chem. Inf. Model.*, 2024, **64**, 3896–3911.
62 P. Pokorná, V. Mlýnský, G. Bussi, J. Šponer and P. Stadlbauer, *Int. J. Biol. Macromol.*, 2024, **26**, 129712.
63 V. M. Yashchuk, V. Yu. Kudrya, I. Ya. Dubey, K. I. Kovalyuk, O. I. Batsmanova, V. I. Mel'nik and G. V. Klishevich, *Mol. Cryst. Liq. Cryst.*, 2016, **639**, 151–159.
64 V. M. Yashchuk and V. Yu. Kudrya, *Methods Appl. Fluoresc.*, 2017, **5**, 014001.
65 V. Yu. Kudrya, V. M. Yashchuk, A. P. Naumenko, Y. Mely, T. V. Udod and Yu. S. Kreminska, *Ukr. J. Phys.*, 2018, **63**, 912–915.
66 V. M. Yashchuk, V. Yu. Kudrya, M. Y. Losytskyy, I. Y. Dubey and H. Suga, *Mol. Cryst. Liq. Cryst.*, 2007, **467**, 311–323.
67 Yu. V. Didan, M. M. Ilchenko, V. V. Negrutska, L. V. Dubey, O. A. Ryazanova and I. Ya. Dubey, *Biopolym. Cell*, 2018, **34**, 387–399.
68 Y. Wang and D. J. Patel, *Structure*, 1993, **1**, 263–282.
69 J.-L. Mergny and L. Lacroix, *Curr. Protoc. Nucleic Acid Chem.*, 2009, **17**, 1–15.
70 M. Gueron, J. Eisinger and R. G. Shulman, *J. Chem. Phys.*, 1967, **47**, 4077–4091.
71 J. Šponer, G. Bussi, P. Stadlbauer, P. Kührová, P. Banáš, B. Islam, S. Haider, S. Neidle and M. Otyepka, *Biochim. Biophys. Acta Gen. Subj.*, 2017, **1861**, 1246–1263.
72 P. Stadlbauer, P. Kührová, L. Vicherek, P. Banáš, M. Otyepka, L. Trantírek and J. Šponer, *Nucleic Acids Res.*, 2019, **47**, 7276–7293.
73 H. Kim, E. Kim and Y. Pak, *J. Chem. Inf. Model.*, 2023, **63**, 6366–6375.